ARTICLE
Journal of Cellular Biochemistry 114:697–707 (2013)

Journal of Cellular Biochemistry

3,4-Dimethoxystilbene, a Resveratrol Derivative With Anti-Angiogenic Effect, Induces Both Macroautophagy and Apoptosis in Endothelial Cells

Lu Zhang,[1*] HongJuan Jing,[1] LiuQing Cui,[1] HuanQing Li,[1] Bo Zhou,[2] GuangZhou Zhou,[1] and Fang Dai[2*]

[1] *College of Bioengineering, Henan University of Technology, Zhengzhou 450001, China*

[2] *State Key Laboratory of Applied Organic Chemistry, Lanzhou University, Lanzhou 730000, China*

ABSTRACT

Angiogenesis plays an important role in many pathological processes. Identification of novel anti-angiogenic agents will provide new insights into the mechanisms for angiogenesis as well as potential lead compounds for developing new drugs. In the present study, a series of resveratrol methylated derivatives have been synthesized and screened. We found trans-3,4-dimethoxystilbene (3,4-DMS) with the fullest potential to develop as an anti-angiogenic agent. In vitro and in vivo analyses suggested that 3,4-DMS could effectively inhibit endothelial cell proliferation, migration, tube formation, and endogenous neovascularization. Our results showed that 3,4-DMS exerted its anti-angiogenic effect likely through induction of endothelial cell apoptosis via a pathway involving p53, Bax, cytochrome *c*, and caspase proteases. Moreover, 3,4-DMS also induced macroautophagy in endothelial cells through activation of AMPK and the downstream inhibition of mTOR signaling pathway. Further studies indicated that intracellular calcium ($[Ca^{2+}]_i$) might bridge the 3,4-DMS-induced apoptosis and macroautophagy through modulating reactive oxygen species (ROS) levels in endothelial cells. Combination of 3,4-DMS with inhibitor of autophagy, such as 3-methyladenine (3-MA) and autophagy-related gene (ATG) 5 small interfering RNA (siRNA), potentiated the pro-apoptotic and anti-angiogenic effects of 3,4-DMS. Our study provides a novel angiogenic inhibitor and a useful tool in exploring the molecular mechanisms for the crosstalk between apoptosis and macroautophagy in endothelial cells. 3,4-DMS could be served as a potential lead compound for developing a class of new drugs targeting angiogenesis-related diseases. J. Cell. Biochem. 114: 697–707, 2013.

KEY WORDS: ANGIOGENESIS; APOPTOSIS; ENDOTHELIAL CELL; MACROAUTOPHAGY; TRANS-3,4-DIMETHOXYSTILBENE

Angiogenesis, the sprouting of new microvessels from pre-existing vasculature, is a tightly regulated process that mainly involves endothelial cell (EC) proliferation, migration, and organization into capillaries [Lamalice et al., 2007]. While physiologic angiogenesis is fundamental for embryonic vascular development, wound healing and organ regeneration, pathologic angiogenesis has been proven as part of the pathogenesis of many diseases, such as solid tumors, atherosclerosis, diabetic retinopathy, and rheumatoid arthritis [Quesada et al., 2006; Dong et al., 2007; Lin et al., 2012]. Since the first angiogenic inhibitor was reported by Taylor and Folkman [1982], an increasing number of anti-angiogenic agents have been discovered and entered into clinical trials [Deplanque and Harris, 2000]. However, serious side effects, such as bleeding, hypertension, and gastrointestinal perforation, have been associated with currently available anti-angiogenic agents, limiting their chronic use [Kamba and McDonald, 2007]. Discovery of new angiogenic inhibitors with novel modes of action and structure will provide new insights into the complicated biology

Additional supporting information may be found in the online version of this article.

Grant sponsor: National Natural Science Foundation of China; Grant numbers: 31101001, 31000580; Grant sponsor: Technological Innovation Incubator Program from Henan University of Technology; Grant number: 11CXRC12; Grant sponsor: Doctoral Scientific Research Start-Up Foundation from Henan University of Technology; Grant number: 2011BS013; Grant sponsor: Fundamental Research Funds for the Central Universities; Grant number: lzujbky-2010-108.

*Correspondence to: Dr. Lu Zhang or Dr. Fang Dai, College of Bioengineering, Henan University of Technology, Zhengzhou 450001, China. E-mail: chaperones@163.com; fangdai@lzu.edu.cn

Manuscript Received: 26 May 2012; Manuscript Accepted: 24 September 2012

Accepted manuscript online in Wiley Online Library (wileyonlinelibrary.com): 11 October 2012

DOI 10.1002/jcb.24411 • © 2012 Wiley Periodicals, Inc.

of angiogenesis as well as a potential lead compound for developing new drugs targeting angiogenesis.

Resveratrol (trans-3,4′,5-trihydroxystilbene; RVT), a naturally polyphenolic phytoalexin found in grapes, has a variety of significant physiological activities including angiogenesis regulation [Chen and Tseng, 2007]. Unfortunately, RVT can induce opposite effects on angiogenesis, either pro- or anti-angiogenic effects, depending on the situation and different cell type [Chen and Tseng, 2007]. In addition, RVT has a low oral adsorption and metabolic stability because it has three hydroxyl groups [Walle et al., 2004]. Structural modifications of the RVT are needed to increase its bioavailability while preserving its beneficial activities. Recently, several studies indicated that RVT methylated derivatives have higher bioavailability and more effective than RVT [Basini et al., 2010; Lin and Ho, 2011]. In our laboratory, a series of RVT methylated derivatives have been synthesized. After screening, we identified trans-3,4-dimethoxystilbene (3,4-DMS, Fig. 1) with the fullest potential to develop as an anti-angiogenic drug.

Increasing evidence suggested that the induction of EC apoptosis may suppress angiogenesis [Chavakis and Dimmeler, 2002]. For example, kringle 5 of human plasminogen (K5), an angiogenic inhibitor, has been shown to induce EC apoptosis [Nguyen et al., 2007]. In the present study, to clarify whether the anti-angiogenic activity of 3,4-DMS is related to apoptosis, we investigated the effect of 3,4-DMS on ECs.

Macroautophagy (herein referred to as autophagy) is a bulk-destruction process in eukaryotes. During this process, the cytoplasm containing long-lived proteins and organelles is engulfed into double-membrane autophagosomes, and ultimately undergoes enzymatic degradation within lysosomes [Yang and Klionsky, 2010]. Autophagy serves as a suicide pathway with complete self-digestion under excessive stress conditions, which is classified as programmed cell death type II [Nguyen et al., 2007]. On the other hand, autophagy has been focused as an adaptive strategy of cell protection against drug-induced apoptosis in normal cells as well as in cancer cells [Kondo et al., 2005; Nishikawa et al., 2010]. By nature, ECs are highly resistant to death inflicted by a wide series of biochemical stimuli [Belloni et al., 2010]. Several anti-angiogenic agents, including K5 [Nguyen et al., 2007] and endostatin [Nguyen et al., 2009], have been shown to specifically evoke an autophagic survival response in ECs. Our present studies showed that 3,4-DMS also induced autophagy in ECs. We were interested in determining whether autophagy played any role during the treatment of ECs with 3,4-DMS.

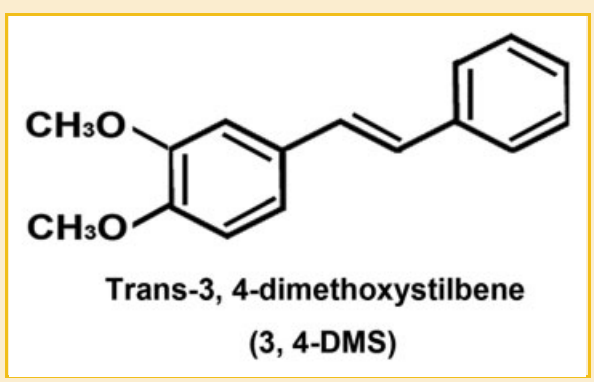

Fig. 1. The chemical structure of 3,4-DMS. 3,4-DMS has a molecular formula $C_{16}H_{16}O_2$ with a molecular weight of 240.2970 g/mol. 3,4-DMS was dissolved in DMSO (0.1 M) as a stock solution.

MATERIALS AND METHODS

CELL CULTURE

Human umbilical vein vascular endothelial cells (HUVECs) were obtained in our laboratory as described [Jaffe et al., 1973]. Cells were cultured on gelatin-coated plastic dishes in M199 medium (Gibco) supplemented with 20% fetal bovine serum (FBS; Hyclone Lab) and 70 ng/ml fibroblast growth factor 2 in a humidified incubator at 37°C with 5% CO_2. Cells at not greater than passage 8 were used. The identity of HUVECs was confirmed by their cobblestone morphology and strong positive immunoreactivity to von Willebrand factor (vWF).

CELL PROLIFERATION ASSAY

HUVEC proliferation was determined by BrdU (bromodeoxyuridine) assay as previously described [Subramanian et al., 2005]. Briefly, cells were incubated with BrdU solution at a final concentration of 0.01 mM for 24 h and then the in situ detection was performed using BrdU In situ Detection Kit (BD Biosciences Pharmingen) according to the manufacturer's instructions. The percentage of proliferating cells was evaluated at a 200× magnification field. A total of 1,000 nuclei were evaluated.

CELL MIGRATION ASSAY

HUVECs were plated in 24-well cell culture plates. Cells were wounded by pipette tips and washed twice with media to remove detached cells. Then, cells were treated with 3,4-DMS (1–40 μM) for 24 h. Migration was documented by photos taken immediately after scraping, as well as 24 h later. Initial and final wound sizes were measured using AxioVision Rel.4.7 software, and difference between the two was used to determine migration distance using the formula: Initial wound size minus final wound size divided by 2.

CAPILLARY-LIKE TUBE FORMATION ASSAY

Growth factor-reduced Matrigel (BD Biosciences, CA) was pipetted into pre-chilled 96-well plates (40 μl Matrigel per well) and polymerized for 1 h at 37°C. HUVECs (4×10^4 per well) in complete media were simultaneously seeded with DMSO (40 μM), 3,4-DMS (10–40 μM), or 3,4-DMS (40 μM) plus 3-methyladenine (3-MA, 10 mM) on Matrigel-coated plates with vascular endothelial cell growth factor (VEGF; 10 ng/ml). After 24 h of incubation, tubular structures were photographed on inverted phase-contrast microscopy (Nikon, Tokyo, Japan) with magnification 100×. The degree of tube formation was quantified by measuring the length of tubes in random fields from each well by use of the National Institutes of Health (NIH) image program.

AORTIC RING SPROUTING ASSAY

Aortas harvested from 8-week-old Sprague–Dawley rats (purchased from Laboratory Animal Center of Zhengzhou University, China) were transversely cut into 1-mm-thick sections. The aortic rings were placed in 96-well plates coated with 40 μl of Matrigel and sealed in place with an overlay of 40 μl of Matrigel. The aortic rings were treated with 3,4-DMS (10–40 μM) for 2 weeks. As a control, aortic rings in VEGF-containing M199 were assayed. The medium were changed every 2 days. The angiogenic sprouting from aortic rings was examined in 30 rings per group (each group rats, $n = 6$). Each aortic ring sprouting was quantified by counting the number of vascular sprouts. All procedures were in accordance with the Guide for the Care and Use of Laboratory Animals published by the US National Institutes of Health (NIH Publication No. 85-23, revised 1996) and was approved by the Animal Care Committee of Henan University of Technology.

CHICK CHORIOALLANTOIC MEMBRANE (CAM) ASSAY

Fertilized chick eggs were kept in a humidified incubator at 37°C for 5 days. After incubation, eggs were opened on the air sac side and chick embryos were prepared by separating the CAM from the shell membrane. Filter disks with DMSO (40 μM), 3,4-DMS (10–40 μM) or 3,4-DMS (40 μM) plus 3-MA (10 mM) were placed on the CAM. The cavity was covered with parafilm, and eggs were incubated for additional 2 days and CAMs were removed for analysis. Angiogenesis was quantified by counting the number of branching blood vessels. Assays for each test sample were carried out using 20 eggs.

CELL VIABILITY ASSAY

HUVECs were plated in 96-well cell culture plates. When cells were grown to 80% confluency, they were washed once with basal M199 medium, incubated with DMSO (40 μM) or 3,4-DMS (40 μM) in completed M199 medium containing VEGF (10 ng/ml) for 24 h. Cell viability was determined by MTT assay as described [Price and McMillan, 1990]. The viability (%) was expressed as = (optical density [OD] of treated group/OD of control group) × 100%. The viability of the control group was set to 100%.

ANALYSIS OF APOPTOTIC CELLS

Chromatin condensation was detected by nuclear staining with Hoechst 33258 (Sigma). After treatment, cells were fixed with 2% formaldehyde for 10 min, stained with 10 μM Hoechst 33258 for 5 min, and then were visualized by fluorescence microscopy (Nikon). Apoptotic cells are stained bright blue because of their chromatin condensation. In addition, apoptotic cells were assessed by terminal deoxynucleotidyl transferase-mediated dUTP nick endlabeling (TUNEL, Promega) according to the manufacturer's protocol. Cells were evaluated by confocal laser scanning microscopy (CLSM, Leica, Germany). The apoptosis rate was quantified by the TUNEL-positive rate.

WESTERN BLOT ANALYSIS

After treatment, HUVECs were lysed in lysis buffer containing 25 mM Tris–HCl (pH 6.8), 2% SDS, 6% glycerol, 2 mM PMSF, 1% β-mercaptoethanol, 0.2% bromphenol blue, and a protease inhibitor cocktail (Sigma) for 10 min on ice and boiled in a digital dry bath incubator for another 10 min. The protein concentration was determined by Coomassie brilliant blue protein assay. Total endothelial protein extracts (30 μg) were applied to 12% SDS–polyacrylamide gel and transferred to a polyvinylidene difluoride (PVDF) membrane (Millipore). Blots were incubated with the corresponding primary antibody (Cell Signaling Technology; 1:1,000) and then with an HRP-conjugated secondary antibody (Santa Cruz Biotechnology; 1:5,000). Band intensity was quantified by use of Quantity one software. Total protein expression was normalized to β-actin levels.

MEASUREMENT OF CASPASE-3 AND CASPASE-9 ACTIVITY

The activities of caspase-3 and -9 were measured according to the kit manufacturers' instructions. Briefly, after treatment, HUVECs were removed from culture dishes and pelleted by centrifugation. Cell pellets were then treated for 10 min with iced lysis buffer supplied with the caspase-3 and -9 assay kits (Calbiochem). Then the suspensions were centrifuged at 10,000*g* for 10 min, and the supernatants were transferred to a clear tube. The specific substrate conjugate [acetyl-Asp-Glu-Val-Asp-*p*-nitroaniline (Ac-DEVD-p-NA) for caspase-3 and acetyl-Leu-Glu-His-Asp-*p*-nitroaniline (Ac-LEHD-p-NA) for caspase-9] was added, and tubes were incubated at 37°C for 2 h. During incubation, the caspases cleaved the substrates to form p-NA. Caspase-3 and -9 activities were read in a microtiter plate reader at 405 nm.

ACRIDINE ORANGE (AO) ASSAY FOR AUTOPHAGY

The volume of acidic vesicular organelles (AVOs), as a marker of autophagy, was detected by staining with lysosomotropic agent acridine orange (Sigma). The cytoplasm and nucleus of the stained cells fluoresced bright green, whereas the AVOs fluoresced bright red. After treatment, cells were stained with AO (5 μg/ml) at 37°C for 1 min and observed by fluorescence microscopy (Nikon).

IMMUNOFLUORESCENCE

After treatment, HUVECs were fixed in 4% paraformaldehyde (w/v) for 30 min at room temperature and blocked in 1× PBS, 0.01% Triton X-100 (v/v), and 5% goat serum (v/v). Cells were subsequently incubated with anti-LC3B antibody (Cell Signaling Technology) overnight at 4°C (cells were incubated with normal IgG for negative controls), and then incubated with Alexa Fluor 488 goat anti-rabbit IgG (Zhongshan Biological Technology) for 1 h. Cells were evaluated by CLSM. Different fields of view (>3 regions) were analyzed for each labeling condition.

MEASUREMENT OF INTRACELLULAR REACTIVE OXYGEN SPECIES (ROS)

After treatment, HUVECs were incubated with CM-H_2DCFDA (5 μM) as a membrane-permeable probe to detect intracellular ROS. After 30 min incubation, fluorescence was detected using a fluorescence microplate reader (FLx800, BIO-TEK) with excitation set at 490 nm and emission detected at 520 nm. Cells were also observed under a CLSM, with an excitation wavelength of 488 nm and an emission wavelength of 530 nm.

DETERMINATION OF INTRACELLULAR CALCIUM ($[Ca^{2+}]_i$) CONCENTRATION

$[Ca^{2+}]_i$ measurements were obtained from HUVECs preloaded with the Ca^{2+}-sensitive fluorescent dye fluo3-acetoxy-methyl ester (Fluo3-AM) by using CLSM. Briefly, cells were loaded with 10 μM Fluo3-AM and 0.02% Pluronic F127 in basic M199 medium for 1 h at room temperature and then normally cultured for 30 min. The fluorescence of Fluo3-AM was excited with an excitation wavelength of 488 nm and fluorescence signals were collected with emission wavelength of 543 nm by CLSM. Data were analyzed with Leica Confocal Software. The $[Ca^{2+}]_i$ was displayed as the intensity of fluorescence relative to that of control at 0 h.

AUTOPHAGY-RELATED GENE (ATG) 5 SMALL INTERFERING RNA (SIRNA) TRANSFECTION

HUVECs at 60% confluence were transiently transfected with ATG5 siRNA by using Lipofectamine™ 2000 (Invitrogen). Briefly, after cells were transfected for 48 h, the medium was replaced with normal M199 medium, and cells were treated with DMSO (40 μM) or 3,4-DMS (40 μM) for 24 h. Scrambled siRNA was used as a negative control. The effect of gene silencing was estimated by Western blot analysis.

STATISTICAL ANALYSES

All experiments were performed in duplicate and repeated at least 3 times. Data are expressed as means ± SE. Treatment groups were compared by *t*-test with SPSS 17.0 (SPSS Inc., Chicago) version. Differences were considered statistically significant at $P < 0.05$.

RESULTS

3,4-DMS INHIBITED HUVEC PROLIFERATION, MIGRATION, AND TUBE FORMATION IN VITRO

Thirty different RVT derivatives were screened for anti-proliferative activity in HUVECs. Cells were exposed to varying doses (1–40 μM) of these compounds and subjected to BrdU assay. Among the derivatives examined, 3,4-DMS (Fig. 1) showed significant anti-proliferative activity. 3,4-DMS treatment (10–40 μM) decreased the HUVEC proliferation by 19.14%, 30.36%, and 48.84%, respectively (Fig. 2A). The data suggested that 3,4-DMS inhibited the proliferation of HUVECs by 50% at a concentration of 46.22 μM (IC_{50}). For this reason, 3,4-DMS was selected as a hit compound for further study.

EC migration is essential for the new blood vessels formation during neo-angiogenesis [Lamalice et al., 2007]. Accordingly, we studied the effect of 3,4-DMS (10–40 μM) treatment on the migratory property of ECs using monolayer cell-wound healing assay. As shown in Figure 2B,C, 3,4-DMS treatment for 24 h inhibited the distance migrated by HUVECs approximately by 28%, 33%, and 56% at 10, 20, and 40 μM, respectively.

Another important step during angiogenesis is the formation and merging of tubes by ECs forming a complex network of vessels and capillaries [Patan, 2004]. The Matrigel tube formation assay serves as an ideal in vitro model system to study the formation of the vascular loop during angiogenesis [Nguyen et al., 2007]. Upon seeding on Matrigel, HUVECs were able to form massive tubelike network in the presence of VEGF for 24 h. Consistent with its effects on proliferation and migration, 3,4-DMS (10–40 μM) markedly reduced the number of branch points, ends, and total tube length in VEGF-induced HUVEC tube formation (Fig. 2D).

3,4-DMS INHIBITED VESSEL SPROUTING EX VIVO AND ANGIOGENESIS IN VIVO

Considering that the effect of 3,4-DMS on HUVECs in vitro cannot be directly translated into its in vivo anti-angiogenic activity, we next assessed whether 3,4-DMS had a direct impact on EC sprouting using the ex vivo rat aortic ring sprouting assay. After 2 weeks, treatment with 3,4-DMS (10–40 μM) suppressed VEGF-induced neovessel sprouting at the cut edge of rat aortic rings compared with the control (Fig. 2E). We further used chick CAM assay to test the anti-angiogenic effect of 3,4-DMS in vivo. In the control chick CAMs, implanted with disks without 3,4-DMS, had no avascular zones in the developing embryos. 3,4-DMS (10–40 μM) induced avascular zones formation. Notably, newly formed microvessels were regressed around the area of 3,4-DMS-implanted disks (Fig. 2F, arrows). This anti-angiogenic activity appeared to be dose-dependent (Fig. 2F). From these data, the most effective does of 3,4-DMS is 40 μM. Thus, all subsequent experiments were performed using 40 μM of 3,4-DMS.

3,4-DMS INDUCED APOPTOSIS IN HUVECs

To elucidate the possible mechanism of 3,4-DMS-induced anti-angiogenesis, we investigated the effect of 3,4-DMS on HUVEC apoptosis. Phase-contrast microscopy was used to evaluate the effect of 3,4-DMS on cell morphological features. Exposure of HUVECs with 3,4-DMS (40 μM) for 24 h increased the number of shrinking cells and cells detached from the culture dish as compared with the control (Fig. 3A). MTT assay revealed that 3,4-DMS (40 μM) significantly reduced the viability of HUVECs (Fig. 3A). The induction of apoptosis was detected with Hoechst 33258 staining and TUNEL assays. Cells incubated with 3,4-DMS (40 μM) for 24 h showed the typical features of apoptosis, including chromatin condensation and nuclear fragmentation (Fig. 3B). The percentage of TUNEL-positive cells in 3,4-DMS treated group was increased by sixfold (Fig. 3C).

We further investigated the mechanism underlying the apoptotic effect of 3,4-DMS. Some studies have demonstrated functional links between p53 expression and EC apoptosis [Zhang et al., 2012]. In our study, Western blot analysis showed that the level of p53 was upregulated in HUVECs incubated with 3,4-DMS (40 μM) for 24 h (Fig. 3D,E). Evidence indicated that p53 accumulation caused the activation of the pro-apoptotic protein Bax, thus leading to the release of cytochrome *c* into cytosol, subsequently activate caspase-9 and -3 and induce EC apoptosis [Munshi et al., 2002]. Treatment with 3,4-DMS (40 μM) for 24 h showed increased Bax expression and cytochrome *c* release (Fig. 3D,E). In addition, 3,4-DMS significantly upregulated the activities of caspase-9 and -3 in HUVECs (Fig. 3F). 3,4-DMS at lower concentrations (10 and 20 μM) could also induce HUVEC apoptosis, but does not exert significant effect as 40 μM (Supplementary Fig. IA–C).

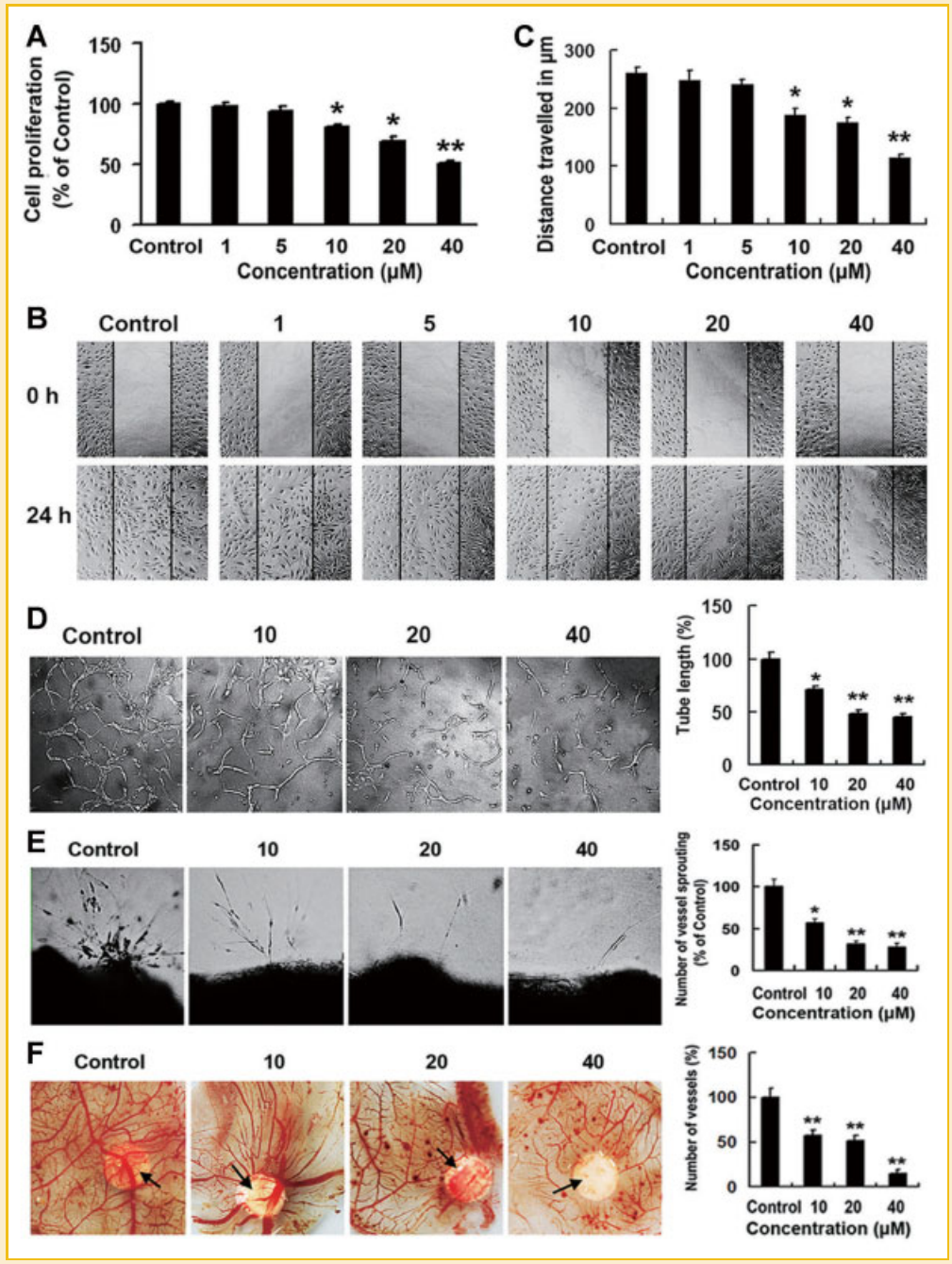

Fig. 2. 3,4-DMS inhibited angiogenesis in vitro, ex vivo and in vivo. A: HUVECs were treated with 3,4-DMS (1–40 μM) for 24 h. Proliferation was then assessed by BrdU assay. B: Effect of 3,4-DMS (1–40 μM) on the migratory potential of HUVEC was analyzed through wound healing assay. Top photos were taken immediately after scraping. Bottom photos were taken after scraping for 24 h. C: Histogram showed the cell migration distance data. D: Effect of 3,4-DMS (10–40 μM) on the tube formation of HUVEC was examined by plating HUVEC on the Matrigel. Histogram showed the total length of tubes. Data are expressed as the mean (±SE) of three independent experiments. E: Effect of 3,4-DMS (10–40 μM) on the EC sprouts formed from the margin of vessel segments from Sprague–Dawley rats. Histogram showed the relative number of vascular sprouts. The angiogenic sprouting from aortic rings was examined in 30 rings per group (each group rats, n = 6). F: Effect of 3,4-DMS (10–40 μM) on the newly formed blood vessels was examined by chick CAM assay. Arrows showed the area of disks. Histogram showed the relative number of newly formed blood vessels on disks. Assays for each test sample were carried out using 20 eggs. $^{*}P < 0.05$, $^{**}P < 0.01$ versus Control.

3,4-DMS INDUCED AUTOPHAGY IN HUVECs

Following 3,4-DMS treatment, HUVECs were stained with AO and observed under a fluorescence microscopy. Cells in control group displayed green fluorescence in cytoplasm and nucleolus, but cells treated with 3,4-DMS (40 μM) for 3 or 6 h showed increased red fluorescent dots in cytoplasm, indicating the formation of AVOs (Fig. 4A). 3,4-DMS at lower concentrations (10 and 20 μM) could also induce the formation of AVOs (Supplementary Fig. ID). Incubating HUVECs with 3,4-DMS (40 μM) for 3 or 6 h markedly increased the number of LC3-positive puncta as compared with the

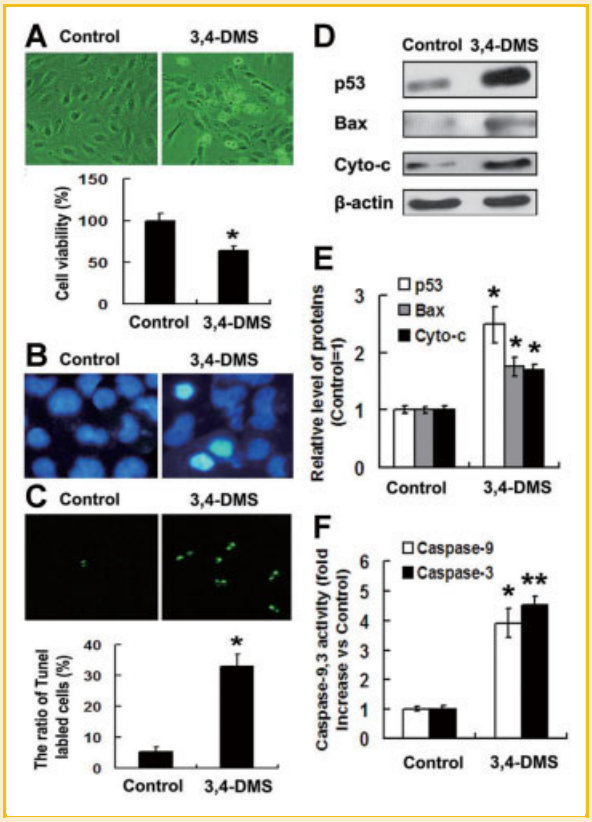

Fig. 3. 3,4-DMS induced HUVEC apoptosis. A: Effect of 3,4-DMS (40 μM) on the cell morphological features (photos) and viability (histogram). B: Cell apoptosis was detected by Hoechst 33258 staining at 24 h. C: Cell apoptosis was detected by TUNEL assay at 24 h. Histogram shows the ratio of TUNEL-positive cells. D: Western blot analysis of p53, Bax, and cytochrome c in response to 3,4-DMS (40 μM) at 24 h. E: Histogram showed the relative levels of p53, Bax, and cytochrome c. F: Effect of 3,4-DMS (40 μM) on the activation of caspase-9 and -3. Data are expressed as the mean (±SE) of three independent experiments. $^{*}P < 0.05$, $^{**}P < 0.01$ versus Control.

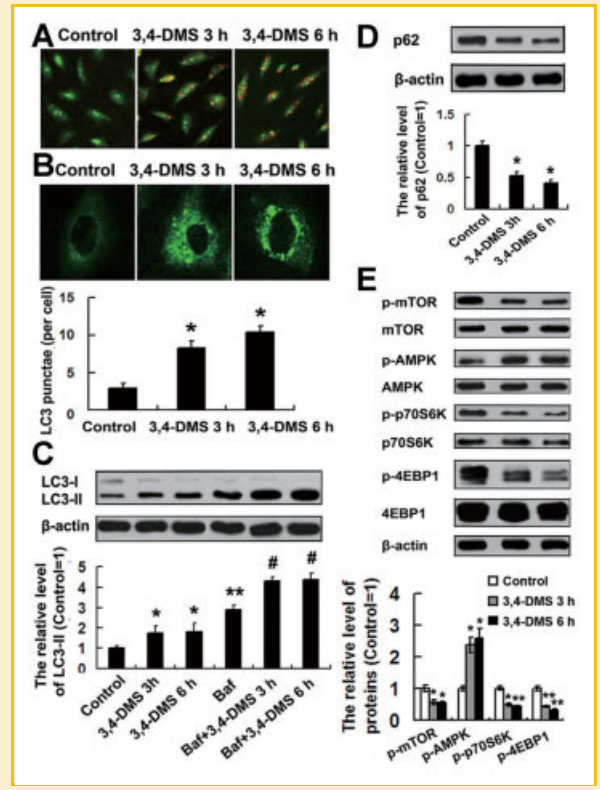

Fig. 4. 3,4-DMS induced HUVEC autophagy. A: AO staining of HUVECs treated with 3,4-DMS (40 μM) for 3 or 6 h. B: Immunofluorescent photographs showed endogenous punctuate of LC3 in HUVECs. Histogram showed the quantification of endogenous LC3 punctuate per cell. C: HUVECs were treated with 3,4-DMS (40 μM) for 3 or 6 h in the presence or absence of bafilomycin A1 (Baf, 100 nM). Western blot analysis of LC3-II accumulation. Histogram showed the relative level of LC3-II. D: Western blot analysis of p62 in HUVECs. Histogram showed the relative level of p62. E: Western blot analysis of the phosphorylation of AMPK, mTOR, p70S6k, and 4EBP1 in HUVECs. Histogram showed the relative levels of these proteins. Data are expressed as the mean (±SE) of three independent experiments. $^{*}P < 0.05$, $^{**}P < 0.01$ versus Control. $^{\#}P < 0.05$ versus Baf.

control, which appeared in similar variation tendency to AO staining (Fig. 4B). We next investigated the effect of 3,4-DMS on LC3 processing and LC3-II accumulation by Western blot analysis. LC3 processing, namely increased ratio of LC3-II/β-actin, was obviously enhanced in HUVECs treated with 3,4-DMS (40 μM) for 3 or 6 h (Fig. 4C). These data suggested that 3,4-DMS might induce autophagy in HUVECs.

However, rather than inducing autophagy, an increase in LC3-II accumulation could instead be due to 3,4-DMS blocking autophagosome fusion with lysosomes and degradation of LC3-II. To determine the mechanism of 3,4-DMS action, we evaluated the autophagic flux in HUVECs. We used bafilomycin A1, a compound prevents fusion of autophagosomes with lysosomes, to demonstrate that 3,4-DMS provoked autophagosome formation. Treatment with bafilomycin A1 (100 nM) increased LC3-II accumulation. Incubating HUVECs with 3,4-DMS (40 μM) and bafilomycin A1 had a more remarkable accumulation of LC3-II (Fig. 4C). Additionally, as a specific substrate for autophagy, p62 is used to monitor autophagic flux [Mizushima et al., 2010]. 3,4-DMS (40 μM) decreased p62 levels obviously (Fig. 4D). 3,4-DMS at lower concentrations (10 and 20 μM) could also induce LC3-II accumulation and p62 decrease in HUVECs, but does not exert significant effect as 40 μM (Supplementary Fig. IE). These data clarified that 3,4-DMS induced autophagy through provoking autophagosome formation instead of causing a blockade of autophagosome/lysosome fusion in HUVECs.

AMPK is a heterotrimeric serine/threonine protein kinase [Fisslthaler and Fleming, 2009]. Vingtdeux et al. [2011] reported a series of structurally related molecules, the resveratrol series, which promoted autophagy by activation of AMPK. Thus, we investigated whether AMPK was involved in 3,4-DMS-induced autophagy. Western blot analysis showed that 3,4-DMS (40 μM) increased AMPK phosphorylation on threonine 172 without affecting the total AMPK levels (Fig. 4E). In the past 7 years, a large number of studies have demonstrated that one of the major downstream signaling pathways regulated by AMPK is the mammalian target of rapamycin (mTOR) signaling pathway [Kim et al., 2011]. Thus, we examined phosphorylation status of mTOR

and its two targets, p70S6K and 4EBP1 after 3,4-DMS treatment. As shown in Figure 4E, 3,4-DMS (40 μM) attenuated phosphorylation of mTOR, p70S6K, and 4EBP1.

$[Ca^{2+}]_i$/ROS WERE INVOLVED IN 3,4-DMS-INDUCED AUTOPHAGY AND APOPTOSIS

In order to dissect the possible mechanism underlying 3,4-DMS-induced apoptosis in HUVECs, we performed a time-course study to determine intracellular ROS, an indicator of oxidative stress which also has been implicated in induction of autophagy [Chen et al., 2009]. 3,4-DMS treatment increased ROS levels within 30 min, and this reached a maximum of 5.4-fold greater than that in 3,4-DMS untreated cells within 360 min (Fig. 5A). We used the potent antioxidant *N*-acetylcystein (NAC) to further examine the involvement of ROS. Pretreatment with NAC effectively reduced the DMS-induced increase in LC3-II levels (Fig. 5B) and TUNEL-positive rate (Fig. 5C,D), indicating that ROS were required for 3,4-DMS-induced autophagy and apoptosis in HUVECs.

To further elucidate the molecular mechanism of 3,4-DMS action, we detected the $[Ca^{2+}]_i$ with the fluorescent dye Fluo3-AM. 3,4-DMS stimulated a rapid and transient increase in $[Ca^{2+}]_i$ followed by a decrease to the level of control cells (Fig. 6A). BAPTA-AM, a chelator of $[Ca^{2+}]_i$, prevented 3,4-DMS-induced increase in ROS levels (Fig. 6B). Furthermore, treatment with BAPTA-AM effectively abrogated the LC3-II accumulation (Fig. 6C) and DMS-induced HUVEC apoptosis (Fig. 6D,E).

3,4-DMS-INDUCED AUTOPHAGY PROLONGED SURVIVAL OF HUVECs

Since autophagy can result in both cell death and survival, we next investigated whether 3,4-DMS-induced autophagy is a process leading to death or a protective response. 3-MA and ATG5 siRNA were used in our experiments to inhibit EC autophagy. Incubating HUVECs with 3,4-DMS (40 μM) alone increased the number of shrinking cells as compared with the control. When cells were treated by the combination of 3,4-DMS (40 μM) with 3-MA (10 mM), this effect was potentiated (Fig. 7A). We next used knockdown of ATG5 by siRNA, which inhibited ATG5 expression by more than 70% after transfection for 48 h (data not shown). Compared with the results in siRNA controls, knockdown of ATG5 enhanced 3,4-DMS-induced detached cells (Fig. 7A). MTT assay revealed that blocking the autophagic response by 3-MA or ATG5 siRNA potentiated the 3,4-DMS-induced decrease of cell viability (Fig. 7B).

TUNEL assay showed that co-treatment with 3,4-DMS and 3-MA significantly increased the proportion of apoptotic cells compared with the cells treated with 3,4-DMS alone (Fig. 7C). Knockdown of

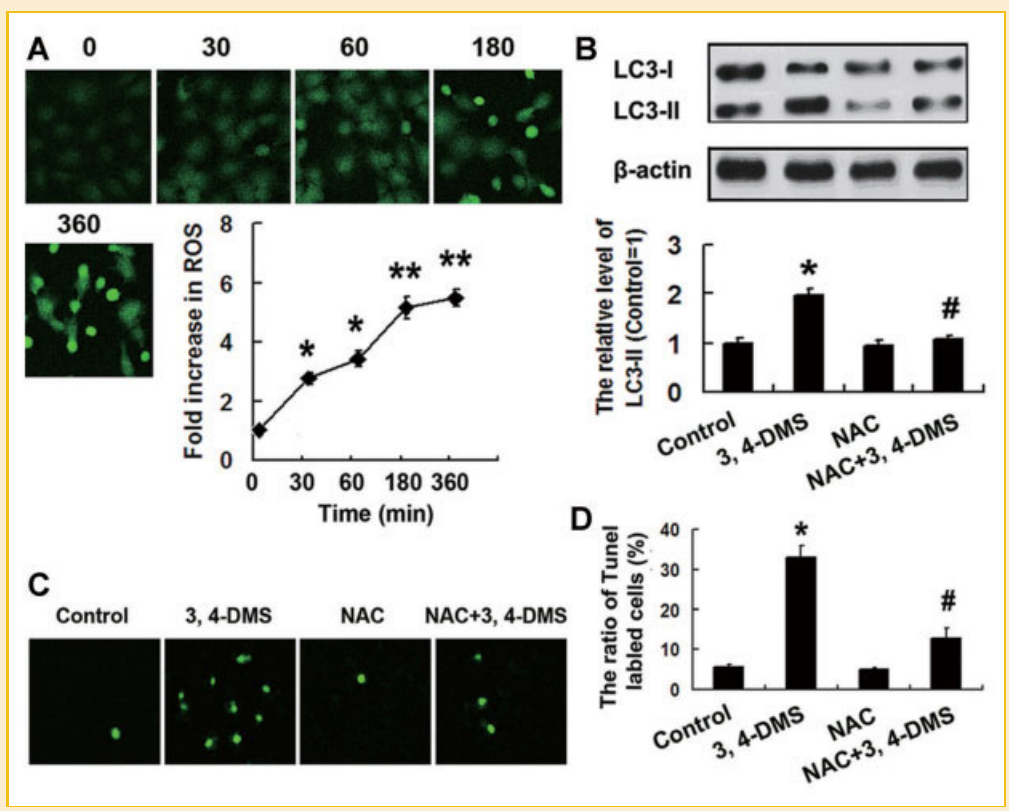

Fig. 5. ROS were involved in 3,4-DMS-induced apoptosis and autophagy. A: The intracellular ROS level was examined by CM-H_2DCFDA (5 μM) after 3,4-DMS treatment (0–360 min). Line chart reflected the relative levels of ROS in HUVECs. B: Western blot analysis of LC3-II accumulation in HUVECs treated with 3,4-DMS (40 μM), NAC (2 mM), or NAC + 3,4-DMS, respectively. Histogram showed the relative level of LC3-II. C: Cell apoptosis was detected by TUNEL assay. D: Histogram shows the ratio of TUNEL-positive cells. Data are expressed as the mean (±SE) of three independent experiments. $^{*}P < 0.05$ versus 0 or Control, $^{**}P < 0.01$ versus 0, $^{\#}P < 0.05$ versus 3,4-DMS.

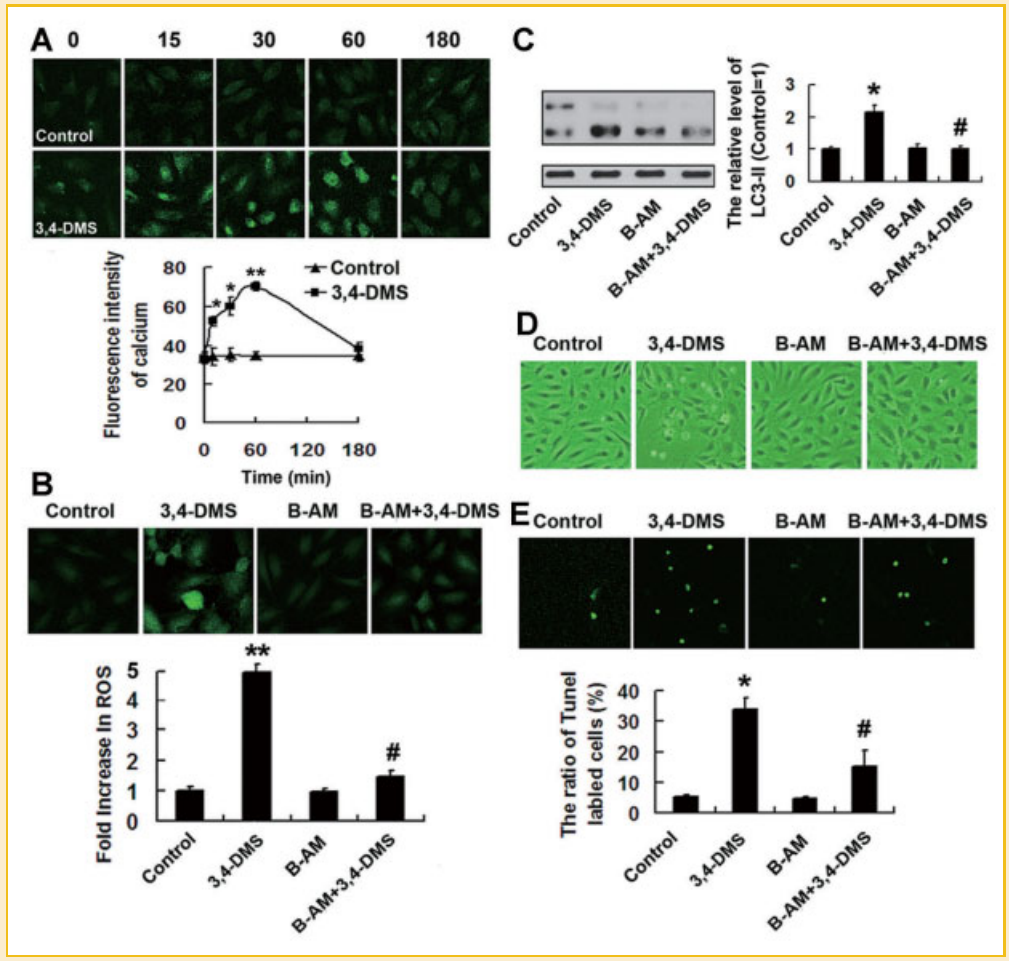

Fig. 6. 3,4-DMS induced HUVEC autophagy and apoptosis through modulating the $[Ca^{2+}]_i$. A: Immunofluorescent photographs reflected the relative levels of $[Ca^{2+}]_i$ in HUVECs treated with or without 3,4-DMS (40 μM) for 0–180 min. Line chart indicated the relative levels of $[Ca^{2+}]_i$. B: The intracellular ROS level was examined by CM-H_2DCFDA in HUVECs treated with 3,4-DMS (40 μM), BAPTA-AM (B-AM, 20 μM) or B-AM + 3,4-DMS, respectively. Histogram reflected the relative levels of ROS in HUVECs. C: Western blot analysis of LC3-II accumulation in HUVECs treated with 3,4-DMS (40 μM), BAPTA-AM (B-AM, 20 μM) or B-AM + 3,4-DMS, respectively. Histogram showed the relative level of LC3-II. D: Co-treatment with B-AM decreased the number of shrinking cells as compared with the 3,4-DMS treated group. E: Cell apoptosis was detected by TUNEL assay. Histogram shows the ratio of TUNEL-positive cells. Data are expressed as the mean (±SE) of three independent experiments. $^{*}P < 0.05$ versus 0 or Control, $^{**}P < 0.01$ versus 0 or Control, $^{\#}P < 0.05$ versus 3,4-DMS.

ATG5 also dramatically enhanced the percentage of TUNEL-positive cells compared with the cells treated with 3,4-DMS alone (Fig. 7C). These data suggested that interfering with autophagy in HUVECs can potentiate the apoptotic effects of 3,4-DMS.

INHIBITION OF AUTOPHAGY POTENTIATED THE INHIBITORY EFFECT OF 3,4-DMS ON ANGIOGENESIS

Finally, we investigated the functional implication of autophagy inhibition and 3,4-DMS treatment in HUVECs. Co-treatment with 3-MA strongly potentiated the inhibitory effect of 3,4-DMS on capillary-like tube formation ability (Fig. 7D). Consistent with the in vitro data, a combination of 3,4-DMS and 3-MA led to a significant reduction in chick CAM angiogenesis compared with the control group (Fig. 7E). Interestingly, 3-MA (10 mM) itself slight suppressed the formation of microvessel structures, which suggested that at some extent HUVECs depend on autophagy for their survival even in normal conditions.

DISCUSSION

Angiogenesis is a significant component of many physiological and pathological states [Crawford et al., 2009; Lin et al., 2012]. The central element in the development of blood vessels are ECs which under control of strictly defined chemical mediators elicit degradation of vascular basement membrane, proliferate and migrate into the perivascular stroma which eventually leads to formation of tubular structures and tissue neovascularization [Coultas et al., 2005]. Since angiogenesis is considered an optimal target for combating neovascularization-dependent diseases, such as tumor and diabetic retinopathy, the research focused on discovering anti-angiogenic agents as a treatment of these serious diseases, is very active. An increasing number of clinically drugs have been developed from natural source, by structural modification of natural compounds or by the synthesis of new compounds designed following a natural compound as model [Gordaliza, 2007].

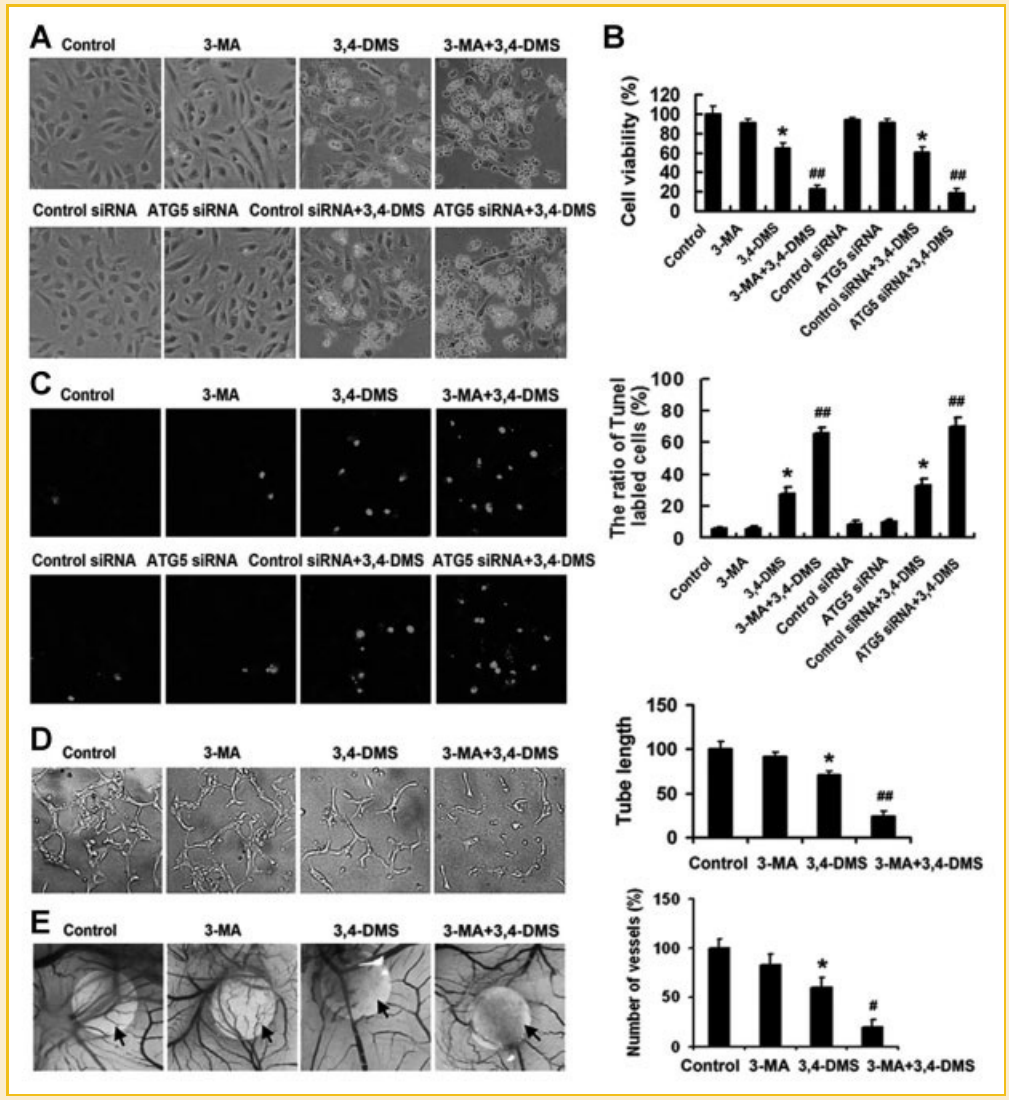

Fig. 7. Inhibition of autophagy potentiated the pro-apoptotic and anti-angiogenic effects of 3,4-DMS. A: Co-treatment with 3-MA (10 mM) or ATG5 siRNA dramatically increased the number of shrinking cells as compared with the 3,4-DMS (40 μM) treated group. B: Cell viability was determined by MTT assay. C: Cell apoptosis was determined by TUNEL assay. Histogram shows the ratio of TUNEL-positive cells. Data are expressed as the mean (±SE) of three independent experiments. D: Co-treatment with 3-MA (10 mM) dramatically potentiated the inhibitory effect of 3,4-DMS (40 μM) on tube formation of HUVECs. Histogram showed the total length of tubes. Data are expressed as the mean (±SE) of three independent experiments. E: Co-treatment with 3-MA (10 mM) markedly potentiated the inhibitory effect of 3,4-DMS (40 μM) on the newly formed blood vessels of chick CAM. Arrows showed the area of disks. Histogram showed the relative number of newly formed blood vessels on disks. Assays for each test sample were carried out using 20 eggs. $^{*}P < 0.05$, 3,4-DMS versus Control, Control siRNA + 3,4-DMS versus Control siRNA. $^{\#}P < 0.05$ versus 3,4-DMS. $^{\#\#}P < 0.01$, 3-MA + 3,4-DMS versus 3,4-DMS, ATG5 siRNA + 3,4-DMS versus Control siRNA + 3,4-DMS.

In the present study, a series of RVT methylated derivatives were synthesized and screened. We found that 3,4-DMS at 10–40 μM effectively inhibited HUVEC proliferation, migration, and tube formation, also strongly inhibited neovessel sprouting at the cut edge of rat aortic ring, as well as suppressed angiogenesis in chick CAMs. These data suggested that 3,4-DMS is an effective anti-angiogenic compound.

Induction of EC apoptosis is an important anti-angiogenic mechanism [Bråkenhielm et al., 2004]. Some agents, such as ceramide, does not appear to induce EC apoptosis, but does inhibit any angiogenic events [Bansode et al., 2011]. In the current study, we have shown that 3,4-DMS could induce apoptosis in HUVECs. Further study showed that 3,4-DMS increased the accumulation of p53 and expression of pro-apoptotic Bax, thus leading to the release of cytochrome *c*, which is critical for activation of the caspase-9 and -3, the final common effector proteases mediating apoptosis signaling in ECs. These observations suggested that the 3,4-DMS-induced EC apoptosis may contribute to its potent anti-angiogenic activity.

It is becoming increasingly evident that ECs activate autophagy as well as apoptosis when they are treated with angiogenic inhibitors [Nguyen et al., 2007; Belloni et al., 2010]. Consensus has not been

achieved concerning the real function of EC autophagy in angiogenesis. Induction of EC autophagy has been recently focused as a mechanism of drug resistance but some report autophagy as a mechanism of cell death in response to therapy. For instance, K5, an angiogenic inhibitor, induced both autophagy and apoptosis in ECs. Interfering with the autophagic survival response increased the anti-angiogenic activity of K5 [Nguyen et al., 2007]. Similarly, the induction of autophagy by another agent, namely sulforaphane (SUL), prolonged survival of ECs. The combination of SUL with specific inhibitor of autophagy potentiated its anti-angiogenic effect [Nishikawa et al., 2010]. On the other hand, Bortezomib, a drug with anti-angiogenic effect, could induce HUVEC autophagy, and blockade of the autophagic pathway prevented Bortezomib-induced cell death, suggesting that Bortezomib-induced autophagy is not a cytoprotective response [Belloni et al., 2010]. In this study, autophagy induction by 3,4-DMS in HUVECs was confirmed by both the accumulation of AVOs and the recruitment of LC3 to autophagosomes in the cytoplasmatic compartment. In addition, Western blot analysis showed that 3,4-DMS treatment increased phosphorylation of AMPK and attenuated phosphorylation of mTOR and its downstream targets, p70S6k and 4E-BP1. It is possible that 3,4-DMS could induce autophagy by AMPK activation and the downstream inhibition of mTOR signaling pathway. Although AMPK is traditionally thought of as a sensor of cellular energy status and a regulator of metabolism, recent discoveries have provided novel evidence that it may function as a protector of endothelial function [Zou and Wu, 2008]. We speculated that 3,4-DMS-induced autophagy as the defense mechanism against apoptosis, which could lead to resistance to anti-angiogenic effect of 3,4-DMS.

Indeed, our experiments have demonstrated that 3,4-DMS-induced autophagy is a protective response, as both pharmacological and genetic inhibition of autophagy significantly potentiated 3,4-DMS-induced HUVEC apoptosis and impaired angiogenesis both in vitro and in vivo. Autophagy might help ECs adapt to and be protected from the cytotoxic effect of 3,4-DMS. The combination of 3,4-DMS with specific inhibitor of autophagy could potentiate the anti-angiogenic activity of this small-molecular compound, and should be a potential new strategy to treat angiogenesis-related diseases.

The signal cross-talk between apoptosis and autophagy is surely critical to the overall fate of the ECs. In the current study, we further explored the factors involved in the association of 3,4-DMS-induced apoptosis and autophagy. Our results showed that 3,4-DMS treatment increased ROS levels. Pretreatment with NAC effectively reduced the 3,4-DMS-induced apoptosis and autophagy in HUVECs. Additionally, treatment with BAPTA-AM, a chelator of $[Ca^{2+}]_i$, blocked 3,4-DMS-induced increase in ROS levels, and effectively suppressed 3,4-DMS-induced apoptosis and autophagy in HUVECs. Numerous studies have provided strong support for a proposal that ROS could act as upstream signal of p53 leading to apoptosis in ECs [Cheng et al., 2007; Liu and Sun, 2010]. More recently, it has been reported that AMPK is required for ROS-triggered autophagy, which increases EC survival in response to cell stress [Wang et al., 2011]. Based on these observations, we speculated that $[Ca^{2+}]_i$/ROS might function in 3,4-DMS-induced apoptosis and autophagy. Further studies to address the molecules that bridge 3,4-DMS-induced apoptosis and autophagy could lead to novel approaches for enhancing the therapeutic efficacy of this angiogenic inhibitor.

Pterostilbene (3,5-dimethoxy-4′-hydroxystilbene; PT) is a naturally occurring analogue of 3,4-DMS found in blueberries and several varieties of grapes [Remsberg et al., 2007]. In our previously study, we found that PT could protect HUVECs from oxidized low-density lipoprotein (oxLDL)-induced apoptosis [Zhang et al., 2012]. In addition, PT (10–40 μM) had no obvious effect on HUVEC proliferation and migration, as well as newly formed microvessels in chick CAMs (Supplementary Fig. II), indicating that PT does not possess anti-proliferative and anti-angiogenic activities as compared with its analog, 3,4-DMS. Interestingly, Chen et al. [2010] have demonstrated that PT induces autophagy and apoptosis in sensitive and chemoresistant human bladder cancer cells. Recently, we also found that PT could promote an increase in functional and cytoprotective autophagy via AMPKα1-mTOR pathway. 3,4-DMS and PT exert different effects on endothelial cells, although both of them possess structural similarity and could induced cytoprotective autophagy. 3,4-DMS appears toxic to endothelial cells and possess anti-angiogenic activity, while PT is an endothelial protective agent and does not have toxicity. These data suggested that the cross-talk between apoptosis and autophagy in endothelial cells is quite complex. Both of these small-molecular compounds would provide novel useful tool in exploring the molecular mechanisms for cross-talk between apoptosis and autophagy.

In conclusion, we have, for the first time, presented evidence that 3,4-DMS was a potential anti-angiogenic agent, by inhibiting the proliferative ability, through induction of EC apoptosis. Furthermore, 3,4-DMS activated autophagy to protect ECs from death. Although several essential connections among apoptosis and autophagy need to be elucidated, our study suggested that blocking the autophagic response will potentiate EC apoptosis and the inhibitory effect of 3,4-DMS on angiogenesis.

ACKNOWLEDGMENTS

This work was financially supported by the National Natural Science Foundation of China (no. 31101001 and no. 31000580), the Technological innovation incubator program from Henan University of Technology (no. 11CXRC12), the doctoral scientific research start-up foundation from Henan University of Technology (no. 2011BS013) and the Fundamental Research Funds for the Central Universities (no. lzujbky-2010-108).

REFERENCES

Bansode RR, Ahmedna M, Svoboda KR, Losso JN. 2011. Coupling in vitro and in vivo paradigm reveals a dose dependent inhibition of angiogenesis followed by initiation of autophagy by C6-ceramide. Int J Biol Sci 7:629–644.

Basini G, Tringali C, Baioni L, Bussolati S, Spatafora C, Grasselli F. 2010. Biological effects on granulosa cells of hydroxylated and methylated resveratrol analogues. Mol Nutr Food Res 54:S236–S243.

Belloni D, Veschini L, Foglieni C, Dell'Antonio G, Caligaris-Cappio F, Ferrarini M, Ferrero E. 2010. Bortezomib induces autophagic death in proliferating human endothelial cells. Exp Cell Res 316:1010–1018.

Bråkenhielm E, Veitonmäki N, Cao R, Kihara S, Matsuzawa Y, Zhivotovsky B, Funahashi T, Cao Y. 2004. Adiponectin-induced antiangiogenesis and anti-

tumor activity involve caspase-mediated endothelial cell apoptosis. Proc Natl Acad Sci USA 101:2476–2481.

Chavakis E, Dimmeler S. 2002. Regulation of endothelial cell survival and apoptosis during angiogenesis. Arterioscler Thromb Vasc Biol 22:887–893.

Chen Y, Tseng SH. 2007. Pro- and anti-angiogenesis effects of resveratrol. In Vivo 21:365–370.

Chen Y, Azad MB, Gibson SB. 2009. Superoxide is the major reactive oxygen species regulating autophagy. Cell Death Differ 16:1040–1052.

Chen RJ, Ho CT, Wang YJ. 2010. Pterostilbene induces autophagy and apoptosis in sensitive and chemoresistant human bladder cancer cells. Mol Nutr Food Res 54:1819–1832.

Cheng J, Cui R, Chen CH, Du J. 2007. Oxidized low-density lipoprotein stimulates p53-dependent activation of proapoptotic Bax leading to apoptosis of differentiated endothelial progenitor cells. Endocrinology 148:2085–2094.

Coultas L, Chawengsaksophak K, Rossant J. 2005. Endothelial cells and VEGF in vascular development. Nature 438:937–945.

Crawford TN, Alfaro DV, III, Kerrison JB, Jablon EP. 2009. Diabetic retinopathy and angiogenesis. Curr Diabetes Rev 5:8–13.

Deplanque G, Harris AL. 2000. Anti-angiogenic agents: Clinical trial design and therapies in development. Eur J Cancer 36:1713–1724.

Dong X, Han ZC, Yang R. 2007. Angiogenesis and antiangiogenic therapy in hematologic malignancies. Crit Rev Oncol Hematol 62:105–118.

Fisslthaler B, Fleming I. 2009. Activation and signaling by the AMP-activated protein kinase in endothelial cells. Circ Res 105:114–127.

Gordaliza M. 2007. Natural products as leads to anticancer drugs. Clin Transl Oncol 9:767–776.

Jaffe EA, Nachman RL, Becker CG, Minick CR. 1973. Culture of human endothelial cells derived from umbilical veins. Identification by morphologic and immunologic criteria. J Clin Invest 52:2745–2756.

Kamba T, McDonald DM. 2007. Mechanisms of adverse effects of anti-VEGF therapy for cancer. Br J Cancer 96:1788–1795.

Kim J, Kundu M, Viollet B, Guan KL. 2011. AMPK and mTOR regulate autophagy through direct phosphorylation of Ulk1. Nat Cell Biol 13:132–141.

Kondo Y, Kanzawa T, Sawaya R, Kondo S. 2005. The role of autophagy in cancer development and response to therapy. Nat Rev Cancer 5:726–734.

Lamalice L, Le Boeuf F, Huot J. 2007. Endothelial cell migration during angiogenesis. Circ Res 100:782–794.

Lin HS, Ho PC. 2011. Preclinical pharmacokinetic evaluation of resveratrol trimethyl ether in Sprague–Dawley rats: The impacts of aqueous solubility, dose escalation, food and repeated dosing on oral bioavailability. J Pharm Sci DOI: 10.1002/jps.22588

Lin C, Wu M, Dong J. 2012. Quercetin-4′-O-β-D-glucopyranoside (QODG) inhibits angiogenesis by suppressing VEGFR2-mediated signaling in zebrafish and endothelial cells. PLoS ONE 7:e31708.

Liu X, Sun J. 2010. Endothelial cells dysfunction induced by silica nanoparticles through oxidative stress via JNK/P53 and NF-kappaB pathways. Biomaterials 31:8198–8209.

Mizushima N, Yoshimori T, Levine B. 2010. Methods in mammalian autophagy research. Cell 140:313–326.

Munshi N, Fernandis AZ, Cherla RP, Park IW, Ganju RK. 2002. Lipopolysaccharide-induced apoptosis of endothelial cells and its inhibition by vascular endothelial growth factor. J Immunol 168:5860–5866.

Nguyen TM, Subramanian IV, Kelekar A, Ramakrishnan S. 2007. Kringle 5 of human plasminogen, an angiogenesis inhibitor, induces both autophagy and apoptotic death in endothelial cells. Blood 109:4793–4802.

Nguyen TM, Subramanian IV, Xiao X, Ghosh G, Nguyen P, Kelekar A, Ramakrishnan S. 2009. Endostatin induces autophagy in endothelial cells by modulating Beclin 1 and beta-catenin levels. J Cell Mol Med 13:3687–3698.

Nishikawa T, Tsuno NH, Okaji Y, Sunami E, Shuno Y, Sasaki K, Hongo K, Kaneko M, Hiyoshi M, Kawai K, Kitayama J, Takahashi K, Nagawa H. 2010. The inhibition of autophagy potentiates anti-angiogenic effects of sulforaphane by inducing apoptosis. Angiogenesis 13:227–238.

Patan S. 2004. Vasculogenesis and angiogenesis. Cancer Treat Res 117: 3–32.

Price P, McMillan TJ. 1990. Use of the tetrazolium assay in measuring the response of human tumor cells to ionizing radiation. Cancer Res 50:1392–1396.

Quesada AR, Muñoz-Chápuli R, Medina MA. 2006. Anti-angiogenic drugs: From bench to clinical trials. Med Res Rev 26:483–530.

Remsberg CM, Yáñez JA, Roupe KA, Davies NM. 2007. High-performance liquid chromatographic analysis of pterostilbene in biological fluids using fluorescence detection. J Pharm Biomed Anal 43:250–254.

Subramanian IV, Ghebre R, Ramakrishnan S. 2005. Adeno-associated virus-mediated delivery of a mutant endostatin suppresses ovarian carcinoma growth in mice. Gene Ther 12:30–38.

Taylor S, Folkman J. 1982. Protamine is an inhibitor of angiogenesis. Nature 297:307–312.

Vingtdeux V, Chandakkar P, Zhao H, d'Abramo C, Davies P, Marambaud P. 2011. Novel synthetic small-molecule activators of AMPK as enhancers of autophagy and amyloid-β peptide degradation. FASEB J 25:219–231.

Walle T, Hsieh F, DeLegge MH, Oatis JE, Jr., Walle UK. 2004. High absorption but very low bioavailability of oral resveratrol in humans. Drug Metab Dispos 32:1377–1382.

Wang Q, Liang B, Shirwany NA, Zou MH. 2011. 2-Deoxy-D-glucose treatment of endothelial cells induces autophagy by reactive oxygen species-mediated activation of the AMP-activated protein kinase. PLoS ONE 6: e17234.

Yang Z, Klionsky DJ. 2010. Eaten alive: A history of macroautophagy. Nat Cell Biol 12:814–822.

Zhang L, Zhou G, Song W, Tan X, Guo Y, Zhou B, Jing H, Zhao S, Chen L. 2012. Pterostilbene protects vascular endothelial cells against oxidized low-density lipoprotein-induced apoptosis in vitro and in vivo. Apoptosis 17: 25–36.

Zou MH, Wu Y. 2008. AMP-activated protein kinase activation as a strategy for protecting vascular endothelial function. Clin Exp Pharmacol Physiol 35:535–545.